Influence of Specific Site Binding on the Interactions between Charged Colloids: A (*N,V,T*) Monte Carlo Study

A. Delville[†]

CRMD, CNRS, 1B rue de la Férollerie, 45071 Orléans, Cedex 02, France

Received: March 22, 2000; In Final Form: August 30, 2000

We used a generalized Monte Carlo sampling of the canonical ensemble to describe ionic condensation and binding on charged interfaces. This procedure includes all ion−ion, site−site, and ion−site long-range electrostatic correlations. It predicts a noticeable influence of the inter particle separation on the degree of ionization of the colloids. As a consequence, the inner and outer face of two disklike particles are not symmetrically ionized at separations less than 100 Å. Because of the resulting asymmetry of counterions condensation, long-range electrostatic attraction is expected to occur between such ionisable or neutralizable particles, even in the presence of monovalent counterions.

I. Introduction

Charged colloids represent a large class of materials used in many industrial applications (food and cosmetic industry, drilling, ...). Their physicochemical behavior (swelling, gelling, ionic exchange, ...) is driven by the long-range electrostatic coupling which is monitored by the spatial extent of their diffuse layer. There is a plethora of theoretical and numerical studies devoted to this problem.[1−45] Reviewing them or giving an exhaustive list of published data is beyond the scope of the present article and readers are referred to recent reviews[1,2] on this topic. To summarize, four classes of approach have been proposed:

First, simulations of the structure and properties of colloidal suspensions were performed by using empirical mean force potential (like Yukawa potential),[3−7] obtained by averaging over the coordinates of the small ions. Such approaches are obviously limited by the validity of the potential, i.e., high dilution for the use of Yukawa potential.

Second, treatments based on numerical solution of the Poisson−Boltzmann equation[8−13] give a good idea of the electrostatic repulsion between charged colloids neutralized by monovalent counterions, but they are inadequate to describe the behavior of colloids in the presence of divalent counterions (i.e. under strong coupling conditions) since they neglect correlation forces.

Third, treatments using integral equations (Modified Poisson−Boltzmann,[19] mean spherical approximation,[20] hypernetted chain, ...[20−24,26]), or numerical simulations (Monte Carlo,[27−37] molecular,[38] or Brownian[39] dynamics) are more appropriate to study highly coupled colloids since they include interionic correlations.

Fourth, more recent treatments based on density functional theory[40−44] appear very promising; however, the validity of some of them is restricted by the approximations involved (like the neglect of interionic correlations and the linearization of Boltzmann law).[41−43]

The first common purpose of all these studies is the determination of the number of neutralizing mobile counterions trapped in the electrostatic well in the vicinity of the charged interfaces, leading to the so-called ionic condensation. The net force between such charged colloids is indeed greatly modulated by their fraction of condensed counterions. In addition to this delocalized ion−interface interaction, solvated condensed counterions may also release one or more solvent molecules from their first solvation sphere and form contact ion pairs[25] with oppositely charged sites at the surface of the colloids. This specific site binding is mainly ignored in usual treatments of intercolloidal interactions in the framework of the primitive model, while it also alters the net electric charge of the colloids and thus their mutual repulsion.

The problem most treated, thanks to its simplicity, concerns the distribution of small counterions and spherical macroions.[3−7,12,17,19,21−22,35−36,40−44] Two other idealized geometries were also considered: infinite cylindrical[10,29−30] or lamellar[11,14,15,20,24,26−28,31−34,39] charged colloids. Only a few recent studies were devoted to real systems such as finite charged disks.[13,16,45] In that context, we have analyzed by Monte Carlo simulations the distribution of counterions between two parallel charged disks[45] and shown how the net interparticle force is monitored by the accumulation of counterions in the interparticle domain.

However, whatever the geometry chosen in all these studies, only two limiting conditions[14] were considered, treating the colloid either as a solid with constant electric surface charge density (Neumann boundary condition)[8,10−14] or constant surface electrostatic potential (Dirichlet boundary condition).[14,24]

While these boundary conditions adequately describe metallic particles (for the latter) or dielectric solids of constant charge (for the former), they are both inadequate to describe the interactions between partially charged colloids with surface sites able either to dissociate or to bind specifically solvated counterions.[46−48] Such weak polyacids or polybases occur frequently in natural (biological membranes, polynucleotides, ...) and synthetic (polyelectrolytes [PMA, ...], metallic oxides ...) polyions.[48]

As long as colligative properties (like osmotic swelling, ionic activity, ...) are concerned, the distinction between ionic condensation and specific site binding appears somewhat academic, since the measured properties are monitored by the fraction of free counterions, whatever the exact nature of their

[†] E-mail: delville@cnrs-orleans.fr.

10.1021/jp001090x CCC: $19.00
Published on Web 10/21/2000

interactions with the charged colloids. By contrast, measurements performed using spectroscopic techniques to determine the degree of solvation of the counterions (like NMR[49] or IR,[50] XRay[51] or neutron scattering[52−54]) or by potentiometric titration[46−48] were able to clearly establish the existence of specific site binding. Numerous models[55−63] have been proposed, generally using mean field theory to treat ion/colloid interactions in some empirical manner, including a large range of apparent binding constants to reproduce the complexity of the experimental data.

By contrast, we keep our model as simple as possible and use (*N*,*V*,*T*) Monte Carlo simulations to include all electrostatic interactions between surface sites, condensed and fixed counterions. This approach thus describes interionic correlations which are responsible for short-range electrostatic attraction between strongly coupled polyions.[23,31−34] We have generalized the classical Monte Carlo sampling procedure of the canonical ensemble to describe specific site binding in addition to the classical ion distribution within the diffuse layers. The purpose of this study is to determine the degree of ionization of partially ionized colloids, describing both the ionic distribution within the diffuse layers around two charged disklike particles and the specific site binding of the counterions on the surface sites of the disks. Since ionic activity is sensitive to colloid and salt concentrations, we monitor the degree of ionization of the disks as a function of their separation and the ionic strength. As shown in this study, the resulting charge variation of the disks has a strong influence on the long-range stability of such ionisable colloids.

II. Methods

A. Monte Carlo Procedure. We use (*N*,*V*,*T*) Monte Carlo simulations to determine the distribution of ions between two parallel disks (diameter 200 Å, thickness 8 Å) immersed in a large cubic simulation cell (volume 27×10^9 Å^3). The counterions are either distributed in the simulation cell or bound on one of the surface sites which are distributed uniformly within a regular network on each basal surface of the disks (see Figure 1). As shown in Figure 1, counterions are attracted in the vicinity of charged particles by the electrostatic potential surrounding each particle, leading to the so-called condensation phenomenon. As shown in Figure 2, the accumulation of counterions increases in the inter- particle domain when two parallel charged disks come close together,[45] because of the overlap of their electrostatic well. One can also note in Figure 2 a net influence of the finite size of the charged disks on the local density of condensed counterions.[45] While ionic activity is the same within the whole simulation cell, the local density at the edge of the disk is lower than at its center[16] because of the local weaker overlap of the electrostatic potentials generated by the two disks. The purpose of this study is to treat both ionic condensation and site binding phenomena by using Monte Carlo simulations.

Each basal surface of the disk is uniformly covered by 384 sites (cf. Figure 1). Two different cases are considered here: all the sites of the same disk are either negatively charged or neutral, but both surface sites interact specifically with a solvated cation to form a chemical bond (with a bond length of 1 Å) either partially neutralizing the electric charge of the disk (for negatively charged sites) or increasing gradually the positive charge of the disk (for neutral sites). As a consequence, the electric charge of the disks varies as a function of the number of chemically bounded cations. Since ion condensation is an increasing function of the electric charge of the colloid, both condensation and binding phenomena are strongly coupled. The affinity of the surface site for solvated cation is fixed by its equilibrium constant. The value of the ion/site equilibrium

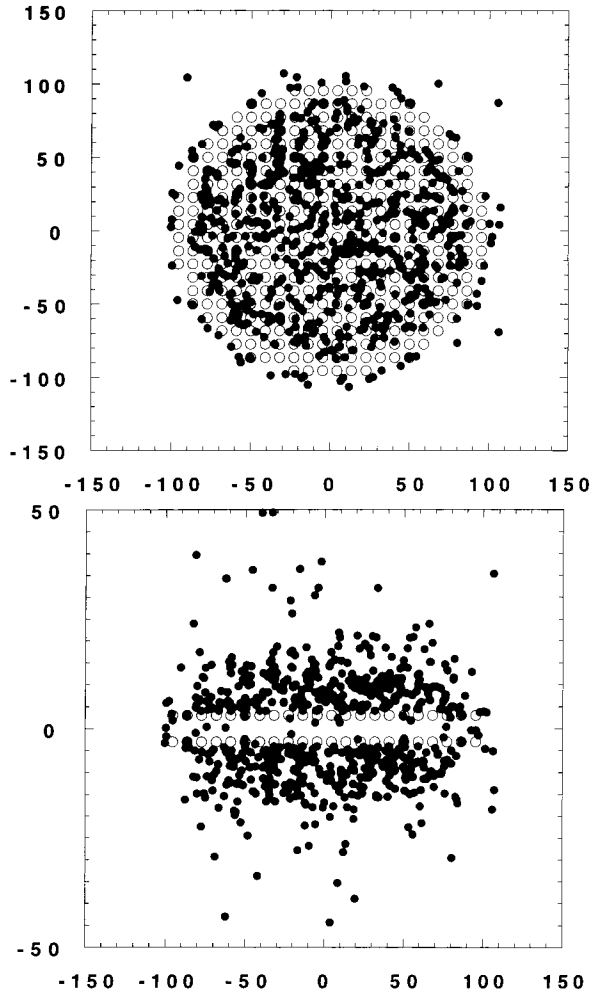

Figure 1. Top (a, upper) and lateral (b, lower) view of a snapshot of one equilibrium configuration of cations (●) either condensed in the vicinity of a charged disk or forming a chemical bond with surface sites (○) distributed at the surface of the disk (see text).

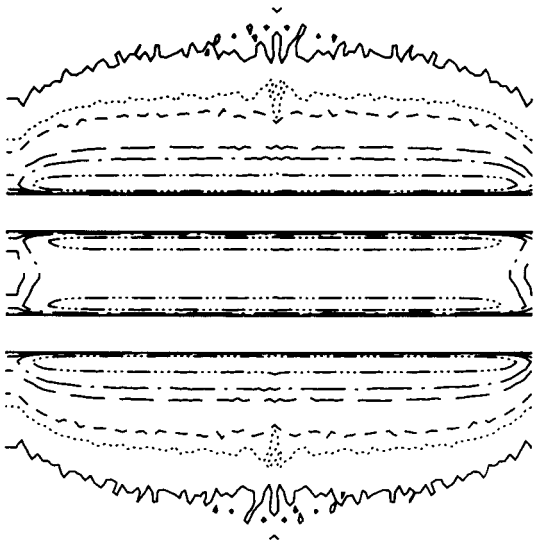

Figure 2. Lateral view of the contour plots of the normalized local concentration (local concentration [*c*(*r*)] divided by the average concentration [*c*°]) of monovalent counterions condensed in the vicinity of two parallel charged disks: $c(r)/c^\circ = 3000$ (—•••—); 1000 (—•—); 500 (—— ——); 100 (- - -), 50 (•••), and 10 (—).

constant is monitored by reference to the standard enthalpy of formation of the chemical bond between *neutral entities* ($\Delta_f H°$) to which electrostatic ion/site interactions are added. The effective surface charge of the disk is calculated as a function of salt concentration of the cell and as a function of the disk separation.

This chemical equilibrium between solvated counterions and a single surface is described within the canonical ensemble by using a generalized partition function:

$$Q(N,V,T) = \sum_{N_{sb}=0}^{N_{st}} \frac{V^{N-N_{sb}}}{\Lambda c^{3(N_c-N_{sb})}\Lambda a^{3Na}} \times \int\int\int \frac{\exp(-E(N_{sb})/kT)}{N_a!\,(N_c-N_{sb})!\,N_{sb}!\,(N_{st}-N_{sb})!}\,dq_1\,dq_i\,dq_N \quad (1)$$

where Λ_i is the de Broglie thermal wavelength of the cations (noted c) or anions (noted a), N is the total number of ions, N_a the total number of anions, N_c the total number of counterions, N_{st} the total number of specific sites, and N_{sb} the number of bonded sites. To mimic proton binding, the mass of both ions is set equal to 1 g/mol.

According to eq 1 and to the microreversibility condition, the probability of forming a new specific ion/site chemical bond on a disk surface which has already bound N_{sb} cations is given by

$$P_{ads} = \min\left\{1, \frac{\Lambda_c^{\,3}(N_c-N_{sb})(N_{st}-N_{sb})\exp(-\Delta E/kT)}{V(N_{sb}+1)}\right\} \quad (2)$$

In the same manner, the probability for an initially bound cation to desorb from a surface with N_{sb} bound cations is given by

$$P_{des} = \min\left\{1, \frac{VN_{sb}\exp(-\Delta E/kT)}{\Lambda_c^{\,3}(N_c-N_{sb}+1)(N_{st}-N_{sb}+1)}\right\} \quad (3)$$

Equations 2 and 3 are written in order to satisfy detailed balance condition.

In order to have an internal probe of the variation of the cation activity as a function of salt concentration or disk separation, we add to the simulation cell two sets of 100 monodisperse indicators (diameter 6 Å), bearing the same electric charge as the surface sites (i.e. negatively charged or neutral) and also able to form a chemical bond with a solvated cation. These indicators behave as dyes (like phenolphthalein) in a colorimetric titration experiment: the variation of their degree of binding gives direct information on any change of the cationic activity. We are obliged to use this means because it is impossible to perform numerical simulations at constant ionic activity. Indeed, we can only fix the activity of neutral entities by using Monte Carlo sampling within the Grand Canonical ensemble. To bypass this problem we chose to monitor the cationic activity by measuring the variation of the affinity of the cations for some reference indicators.

Note that eqs 1−3 are easily generalized in order to thermalize the location of the indicators and their degree of cation binding. Because of the large difference between the indicator and cation mass, we use the same de Broglie thermal wavelength for the free and bound indicators.

Equations 1−3 are used to describe the chemical equilibrium between the solvated counterions and the four surfaces of the disks and the 200 indicators included in the simulation cell. For that purpose, we select randomly, with an equal probability, between three different individual motions: ion displacement, cation binding, and cation desorption.

In the first step, we apply, as usual, a random displacement to any solvated entity (cations, anions, indicators). In the second step, we select randomly one solvated counterion (whatever its location in the simulation cell) plus one available binding site (either located on a disk surface or a indicator) and try to adsorb this cation. The new location is accepted according to eq 2. Note that the energy variation (ΔE) in eq 2 includes not only the change of the electrostatic energy but also the enthalpy of binding ($\Delta_f H°$). In the final step, we select randomly one bound cation (located either on the disk surface or on a indicator) and we try to place this cation randomly within the simulation cell. Equation 3 defines the acceptance probability for this motion. Since, at equilibrium, cation activity is the same everywhere in the cell, adsorption is not limited only to those counterions which are located in the vicinity of the binding sites, nor is it necessary that desorbed counterions be in the vicinity of the original binding site.

Block averages are used to reduce the statistical noise. Typical Monte Carlo simulations are performed with 3000 blocks of 10000 iterations for both the thermalisation and the production steps.

B. Electrostatic Energy. All electrostatic interactions (including ion−ion, site−site, and ion−site interactions) are described in the framework of the primitive model:

$$u_{ij}(r_{ij}) = \frac{q_i q_j}{4\pi\epsilon_0\epsilon_r r_{ij}} \quad (\text{if } r_{ij} \geq a_{ij}) \quad (4a)$$

$$u_{ij}(r_{ij}) = \infty \quad (\text{otherwise}) \quad (4b)$$

The ion diameter (a_{ij}) is set equal to 2 Å. The electrostatic energy is calculated using Ewald summation[64] with classical 3D minimum image convention and periodic boundary condition

$$E_{elect} = E_{dir} + E_{self} + E_{mom} + E_{rec} \quad (5a)$$

$$E_{dir} = \frac{0.5}{4\pi\epsilon_0\epsilon_r}\sum_{\alpha=1}^{N_\alpha}\sum_{i=1}^{n_i} q_{\alpha_i}\sum_{\beta\neq\alpha}^{N_\beta}\sum_{j=1}^{n_j}\frac{q_{\beta_j}\,\mathrm{erfc}(\kappa r_{\alpha_i\beta_j})}{r_{\alpha_i\beta_j}} \quad (5b)$$

$$E_{self} = -\frac{\kappa}{4\pi^{3/2}\epsilon_0\epsilon_r}\sum_{\alpha=1}^{N_\alpha}\sum_{i=1}^{n_i} q_{\alpha_i}^{\,2} - \frac{0.5}{4\pi\epsilon_0\epsilon_r}\sum_{\alpha=1}^{N_\alpha}\sum_{i=1}^{n_i} q_{\alpha_i}\sum_{j\neq i}^{n_j}\frac{q_{\beta_i}\,\mathrm{erf}(\kappa r_{\alpha_i\beta_i})}{r_{\alpha_i\beta_i}} \quad (5c)$$

$$E_{mom} = \frac{2\pi}{V(1+e_\infty)4\pi\epsilon_0\epsilon_r}\left\{\sum_{\alpha=1}^{N_\alpha}\sum_{i=1}^{n_i} q_{\alpha_i}\mathbf{r}_{\alpha_i}\right\}^2 \quad (5d)$$

$$E_{rec} = \frac{2\pi}{V4\pi\epsilon_0\epsilon_r}\sum_{|\mathbf{K}|\neq 0}\frac{\exp(-K^2/4k^2)}{K^2} \times \left[\left\{\sum_{\alpha=1}^{N_\alpha}\sum_{i=1}^{n_i} q_{\alpha_i}\cos(\mathbf{K}\mathbf{r}_{\alpha_i})\right\}^2 + \left\{\sum_{\alpha=1}^{N_\alpha}\sum_{i=1}^{n_i} q_{\alpha_i}\sin(\mathbf{K}\mathbf{r}_{\alpha_i})\right\}^2\right] \quad (5e)$$

where e_∞, the dielectric constant of the continuum surrounding the replica of the simulation cell, is set equal to 1. The index α describes the different entities (ions, indicators, or adsorbing disks), while the running index i describes the different charged

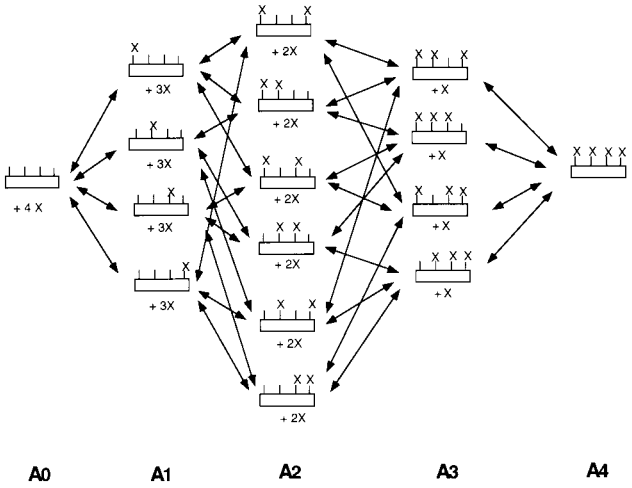

Figure 3. Illustration of the different pathways corresponding to the binding and the desorption of a ligand (X) to/from the four available sites of a substrate (see text).

sites of each disks, *including their bound counterions*. The screening parameter κ is set to 0.006 Å^{-1} and the summation over the reciprocal space is cut for $|\mathbf{K}| \geq 7 \cdot 2\pi/L$, where L is the length of the simulation cell. Since this length is 3000 Å, the limitation on the summation in the reciprocal space leads to an accuracy better than 0.005 for the electrostatic energy.[65] Note that this electrostatic energy also includes the electrostatic interaction between a bound cation and its binding sites on the disk surfaces or with the indicators.

The total energy of each configuration is given by

$$E_{\text{tot}} = E_{\text{elect}} + \sum_{\alpha} N_{\text{sb}\alpha} \Delta H^{\circ} f_{\alpha} \tag{6}$$

where $N_{\text{sb}\alpha}$ is the total number of bound sites on the entity α (disk surface or indicator).

Since the size of the simulation cell (3000 Å) is larger than the maximum separation between the parallel disks (∼500 Å) or the disk diameter (200 Å), the electrostatic energy of a given configuration of the ions is independent of the size of the simulation cell. However, as predicted by Le Chatelier, varying the size of the simulation cell and thus the concentration of the suspension modifies the equilibrium value of the degree of binding of the cations. This Le Chatelier's behavior is the direct consequence of the factor V in eqs 2 and 3.

C. Analysis of the Binding Cooperativity. Because of the long range of the Coulomb potential and of the small minimum separation (∼9 Å) between the binding sites of each disk surface, one expects a strong influence of the surface degree of cation binding on its affinity for the counterions. We use the Hill plot procedure to quantify this so-called cooperativity phenomenon.[55] To simplify, let us consider the case of a substrate bearing four equivalent sites, each able to form a chemical bond with the cations (whose equilibrium concentration is noted $[X_f]$ in Figure 3). Each step of this binding mechanism may be analyzed separately, introducing four apparent binding constants K_i:

$$K_i = \frac{[A_i]}{[A_{i-1}][X_f]} \tag{7}$$

where $[A_i]$ is the equilibrium concentration of the substrates with i bounded cations whatever their location (cf. Figure 3). The substrate degree of binding or saturation function is defined as

$$\theta = \frac{[A_1] + 2[A_2] + 3[A_3] + 4[A_4]}{4([A_0] + [A_1] + [A_2] + [A_3] + [A_4])} \tag{8}$$

But if the four sites are equivalent at each step of the binding mechanism (cf. Figure 3), they have the same chemical affinity for the cations. As a consequence, one may introduce equilibrium constants describing the chemical affinity of the *individual* site by using the appropriate statistical factors:[55]

$$K_1 = \frac{4}{1} k_1$$

$$K_2 = \frac{3}{2} k_2$$

$$K_3 = \frac{2}{3} k_3$$

$$K_4 = \frac{1}{4} k_4 \tag{9}$$

As shown in Figure 3, the formation on the first chemical bond leads to four different realizations of the first substrate/cation complex which are characterized by the same saturation fraction of the substrate and noted as a single chemical species (A_1), but it results from the occurrence of four equivalent binding pathways, each with only one reverse pathway, corresponding to cation desorption (cfr Figure 3). The next step of the substrate/cation binding process leads to the formation of six different realizations of the same chemical entity characterized only by its saturation fraction (A_2). Three independent pathways remain possible for the formation of the second chemical bond, while two different pathways are possible for the backward process (Figure 3). And so on for the two remaining steps (Figure 3).

Let us now generalize and consider a substrate with N binding sites. Its degree of binding is characterized by the generalized partition function[55]

$$\begin{aligned} \xi &= \sum_{i=0}^{N} K_1 \ldots K_i [X_f]^i \\ &= \sum_{i=0}^{N} \frac{N!}{i!(N-i)!} k_1 \ldots k_i [X_f]^i \end{aligned} \tag{10}$$

where the intrinsic binding constants (k_i) are defined as above from the apparent binding constants (K_i) by respectively counting, at each degree of binding, the number of possible pathways for ion binding and desorption.

The degree of binding (eq 8) is directly derived from this partition function:

$$\theta = 1/N \frac{\mathrm{d} \ln \xi}{\mathrm{d} \ln [X_f]} \tag{11}$$

In the absence of any cooperativity, all the intrinsic binding constants are equal and do not vary as a function of the degree of binding of the substrate ($k_i = k$).[55] Thus $\xi = (1 + k[X_f])^N$, which leads to $\theta = k[X_f]/(1 + k[X_f])$. As a consequence, the Hill plot,[66] i.e., the plot of $\ln\{\theta/(1-\theta)\}$ as a function of the logarithm of the equilibrium activity of reactants ($\ln[X_f]$), is a straight line of unit slope whose intercept with the line $\theta/(1-\theta) = 1$ defines the intrinsic binding constant k (cf. Figure 4). By contrast, if the intrinsic binding constants are decreasing functions of the degree of binding ($k_1 > k_i > k_N$) the cooperativity is negative[55] (also called anticooperativity)[55] and the Hill plot deviates strongly from a straight line of unit slope.

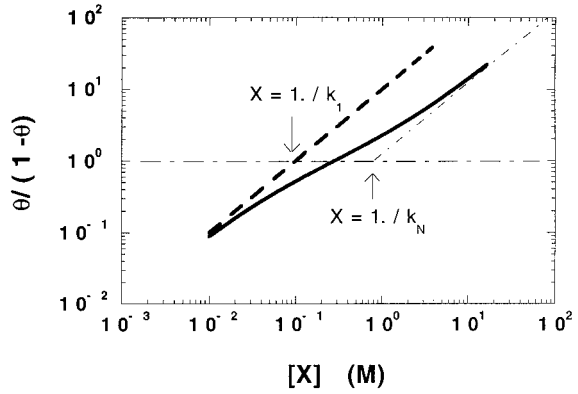

Figure 4. Hill plots used to analyze the cooperativity during the binding of four ligands (X) to a macromolecule under respectively noncooperative ($k_i = 10$, - - -) and anticooperative ($k_1 = 10$, $k_2 = 5$, $k_3 = 2.5$, $k_4 = 1.25$, —) regime.

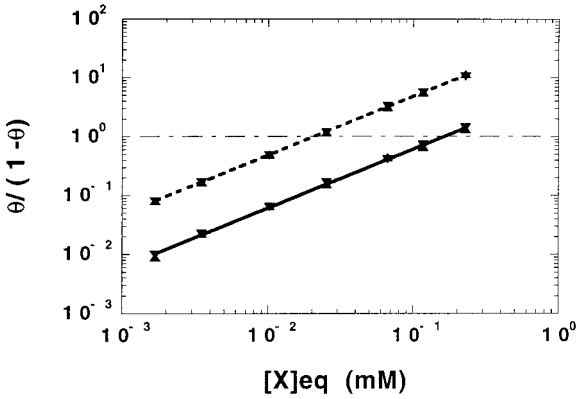

Figure 5. Hill plots describing the degree of binding of neutral solute (X) on two sets of neutral surface sites and solvated indicators (see text) with common standard enthalpy of binding ($\Delta_f H° = -40$ kJ/mol, - - -) and ($\Delta_f H° = -45$ kJ/mol, —)

Note that the slope at $\theta = 0.5$ (the so-called half saturation point) is then smaller than one (see Figure 4) and that the asymptotic lines at low and high degree of binding define respectively the intrinsic binding constants k_1 and k_N. In the case of proton binding to a polyacid, the range of pH values included between such two limiting binding constants defines the range of apparent pK_a of the polyacid.

Preliminary simulations are first performed with all neutral entities (no electrostatic interactions), in order to check the numerical procedures. The two disks are parallel to each other, with a separation of 500 Å. We use the same standard enthalpy of binding for one set of 100 indicators and for the 768 sites located on a same disk (see Figure 1). The intrinsic binding constant of the sites of the two disks are set equal to −40 and −45 kJ/mol, respectively. As shown in Figure 5, the corresponding Hill plots do not exhibit any cooperativity, with a perfect matching of the degree of binding of the equivalent sets of indicators and surface sites because of the absence of lateral interactions between the particles bound on the disks. In this case, the location of the fixation sites has no influence on the degree of binding. The intercepts of these Hill plots define the intrinsic equilibrium constants of both classes of sites: 6.09 and 48.31 M^{-1}, respectively. Since the standard entropies of binding are the same, the ratio of the equilibrium constants, i.e., the difference of their binding free energies, agrees perfectly with the difference of their standard enthalpies of binding. Note that their common standard entropy of binding ($\Delta_f S° \sim -14.3R$) has the same order of magnitude as the entropy difference resulting from the loss of translational entropy of a perfect gas (as evaluated by the Sackur−Tetrode equation) plus the mixing entropy of perfect gases ($\Delta S = -10.6R$).

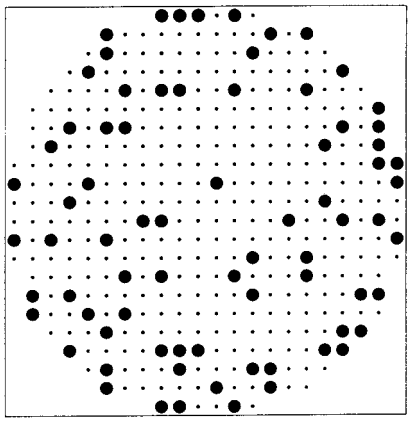

Figure 6. Snapshot of one equilibrium configuration of cations bound at the surface sites of a neutral disk.

III. Results and Discussion

A. Surface Ionization. Let us first consider the ionization of two parallel neutral disks with surface sites able to bind specifically cations with an intrinsic affinity defined by a standard enthalpy of binding ($\Delta_f H°$) equal to −80 kJ/mol. The center to center separation of the disks is 20 Å and they are immersed in a salt solution with total concentrations varying between 0.006 and 0.12 mM. In addition to the salt, the solution contains neutral indicators at concentration 0.012 mM, also able to specifically bind cations, with a standard enthalpy of binding ($\Delta_f H°$) equal to 45 kJ/mol. Both surface sites and indicator affinities are selected to obtain degrees of binding around 50% in order to reduce the statistical noise.

The long-range electrostatic repulsion between the cations is responsible for border effects (cf. Figure 6); all free sites at a surface of the disks are not equivalent: they do not have the same intrinsic binding constant because their affinity for solvated counterions is strongly related to the ionization state of the neighboring sites. As a consequence, the ionization process occurs preferentially at the periphery of the disks to minimize the electrostatic repulsions between ionized sites. This ionic *correlation* is described by the Monte Carlo procedure and will not be detected in a mean field treatment of ionic condensation and binding which is only able to treat the *averaqe* ionization of the colloids.

Furthermore, the cationic affinity of the sites varies as a function of the average degree of binding of the disks. The Hill plot (Figure 7) exhibits negative cooperativity (the slope at half saturation is smaller than one) since preliminary binding of cations strongly reduces the cationic affinity of free sites at the surface of the disks. As a consequence, the apparent degree of binding cannot be reproduced by a single binding constant, and the intrinsic binding constant defined by the standard binding enthalpy is only detected at the initial step of the ionization process.

It is a fact that the ionic activity in the solution cannot be simply deduced from the average equilibrium concentration since ionic condensation greatly modifies the ionic activities in suspensions of charged colloids. We use the degree of binding of the indicators as an inner probe of the variation of cationic activity as a function of salt concentration. The Hill plot describing indicator binding is perfectly linear with a unit slope (Figure 7), corresponding to a noncooperative binding (see above). Introducing activity coefficients to translate the equi-

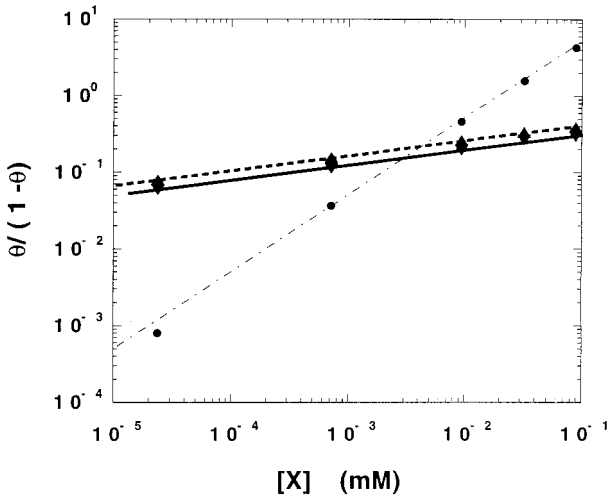

Figure 7. Hill plots describing the degree of binding of two neutral disks resulting from the binding of monovalent cations (X^+). The standard enthalpy of binding ($\Delta_f H°$) is −80 kJ/mol for the surface sites (▼, inner faces; ▲, outer faces) and 45 kJ/mol for the reference indicators (●) (see text).

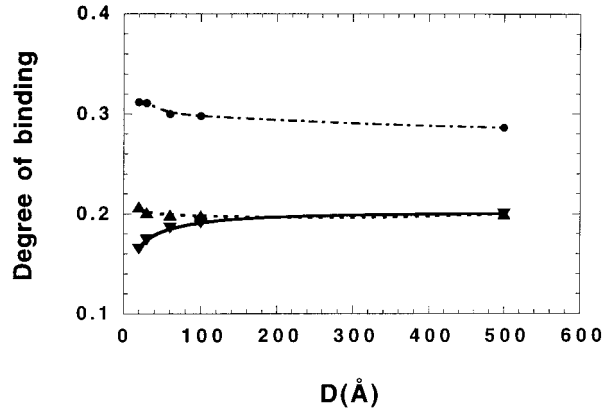

Figure 8. Degree of binding of two neutral disks as a function of their separation under the same conditions as for Figure 7: ▼, inner faces; ▲, outer faces ($\Delta_f H° = -80$ kJ/mol); and ●, indicators ($\Delta_f H° =$ 45 kJ/mol).

librium concentrations of the solutes into their activities, we obtain

$$\theta = \frac{[XD]_{eq}}{[D]_{eq} + [XD]_{eq}} = \frac{K[X]_{eq}\,\gamma_D\gamma_X/\gamma_{XD}}{1 + K[X]_{eq}\gamma_D\gamma_X/\gamma_{XD}} \qquad (12)$$

where $[D]_{eq}$ denotes the equilibrium indicator concentration and $[X]_{eq}$ the equilibrium cation concentration. Assuming $\gamma_D \sim 1$, as expected for a neutral solute in the dilute regime, the linearity of the indicator Hill plot results from the equivalence between γ_X and γ_{XD}, since these dilute solutes bear the same electric charge. Thus, lateral long-range electrostatic interactions between ionized surface sites are responsible for the large difference between the Hill plots describing the degree of binding of the indicators and the surface sites.

Finally, Figure 7 also exhibits systematic differences between the degree of binding of the sites located on the inner and outer faces of the disks: in all cases, the sites located at the inner face of one disk display a lower cationic affinity than the sites located at the outer face because of the influence of the electrostatic potential generated by the second disk which bears the same electric charge. As shown on Figure 8, the minimum separation necessary to detect this difference is of the order of

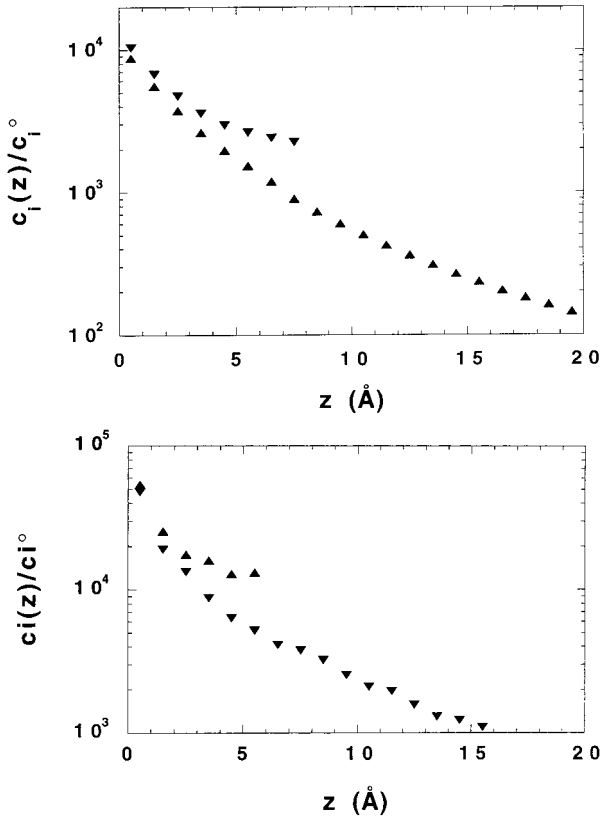

Figure 9. Local densities of counterions condensed in the vicinity of the outer (▲) and inner (▼) surfaces of two parallel disks either without (Figure 9a) or with cation binding (Figure 9b).

100 Å. Here also we use the variation of the degree of binding of the indicators as a probe of any variation of the cationic activity during the decrease of the disk separation. Because of the parallel variation of the degree of binding of the indicator and the outer sites, one may conclude that the charge imbalance between the inner and outer faces of the disks originates from the decrease of the cationic affinity of the inner sites.

This charge imbalance may have a crucial influence on the stability of colloids able to form such chemical bond with some counterions. Indeed, previous Monte Carlo simulations[45] of the ionic condensation of monovalent counterions around two parallel charged disks have shown that the local density of counterions at contact with the disk surface [noted $c(0)$ in eq 13] is not the same on both sides of the disks.[45] Because of the overlap of the electrostatic wells in the vicinity of each disk, the local density of counterions in the inner domain limited by the two disks is larger than the local density outside the disks (cf. Figure 9a). Furthermore, the net repulsion between the disks results mainly from the contribution of the counterion contact force. For monovalent counterions, the contribution of the electrostatic forces remains negligible, and the net repulsion between the disks is given by the balance[45] between the inner and outer contact forces generated by the counterions condensed in contact with the surface of the disks:

$$P_{contact} = kT\{c(0)_{inner} - c(0)_{outer}\} \qquad (13)$$

As a consequence, because of the charge imbalance shown on Figure 8, we expect to cancel the contact pressure, or at least reduce the accumulation of counterions in the inner domain. The concentration profiles shown in Figure 9b still exhibit an average counterion density higher in the inner domain than outside the disks. However, the contact densities on both sides

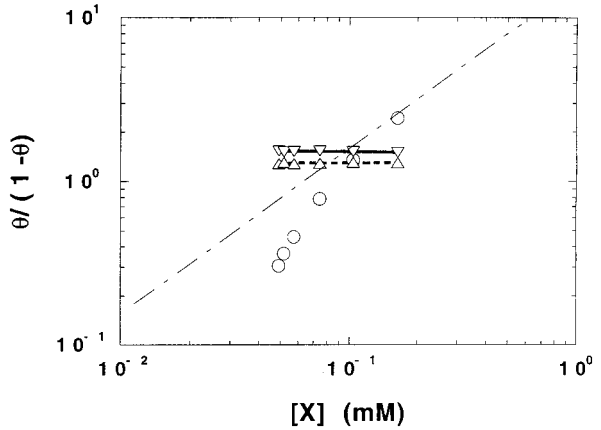

Figure 10. Hill plots describing the degree of binding of two charged disks resulting from the binding of monovalent cations (X^+). The standard enthalpy of binding ($\Delta_f H°$) is 30 kJ/mol for the surface sites (▽, inner faces; ▽, outer faces) and −30 kJ/mol for the reference indicators (○) (see text).

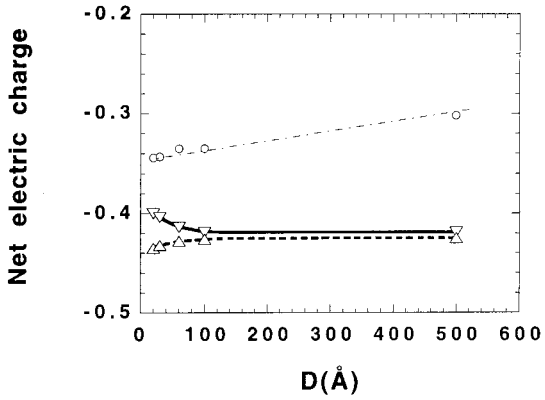

Figure 11. Net electric charge of two negatively charged disks as a function of their separation under the same conditions as for Figure 10: ▽, inner faces; △, outer faces ($\Delta_f H° = 30$ kJ/mol); and ○, indicators ($\Delta_f H° = -30$ kJ/mol).

of the disks become similar, canceling the contact pressure calculated in eq 13. Obviously, further simulations at other disk separations are required to fully confirm these results and determine the contribution of the electrostatic terms to the net inter particle force when colloidal surface sites are able to form a chemical bond with solvated counterions. Nevertheless, we expect such surface ionization to be responsible for the canceling of the net repulsion between charged colloids neutralized by monovalent counterions.

The contribution of the solvent molecules is neglected in the framework of the primitive model. We assume that the contact pressure exerted by the solvent molecules is the same at both sides of the disk. Because of the layering of polar solvent[67−69] at the surface of charged colloids, this approximation is valid if the disk separation is larger than a few (4−6) solvent diameters. This requirement is satisfied in water for disk separations larger than 20 Å, the minimum separation considered here.

B. Surface Neutralization. The second system considered here is the neutralization of two charged disk by formation of a chemical bond between solvated counterions and the monovalent and negatively charged surface sites of the disks. The indicators used to monitor the variation of the cationic activity are also electrically charged, with the same electric charge as the surface sites. In order to keep the degree of binding to about 50% of both disk surface sites and indicators, the standard enthalpy of binding ($\Delta_f H°$) of the surface sites and the indicators are set equal to 30 and −30 kJ/mol, respectively. Because of the strong electrostatic attraction between the counterions and the charged disks, we were obliged to reduce the cationic affinity of the surface sites as compared to that of the monovalent indicator. However, the strong affinity of the surface sites gradually reduces as a function of the degree of binding of cations on the surface, leading again to a negative cooperativity (Figure 10). Because of the long range of the electrostatic coupling, the degree of cation binding of a negative surface sites modifies the affinity of other surface sites at large distance, leading to a nearly flat Hill plot (see Figure 10).

Here also, the ionization degree of the inner and outer faces of the disks differs somewhat: more counterions are bound on the inner faces of the disks, reducing again the local surface charge density and thus the amount of counterions condensed in contact with the inner surface of the disks. As a consequence, the contact contribution to the swelling pressure cancels out (cf. eq 13) and may lead to net attractions between charged colloids with surface sites able to from a chemical bond with monovalent counterions.

The reference Hill plot characterizing the cation binding of the negative indicators also deviates from the straight line of unit slope, suggesting some positive cooperativity (Figure 10). This effect results from the difference between counterion activity and average equilibrium concentration. Indeed, in that case, in eq 12, $\gamma_{XD} \sim 1$ but no cancellation occurs between γ_X and γ_D. By contrast, their product is equal to the square of the corresponding salt activity coefficient, which becomes insensitive to condensation phenomena only at high ionic strength as shown on Figure 10. This deviation from unity of the counterion activity coefficient does not cancel the above-mentioned anticooperativity of the counterion binding to the surface sites but, on the contrary, amplifies it.

Figures 11 also exhibits the influence of the disks separation on the degrees of binding of both their innner and outer surface sites. Here also, a separation smaller than 100 Å is required to detect a notable difference between both degree of cation binding and thus net electric charges of the disk surfaces. This result suggests once more the possibility of long-range electrostatic attraction between partially neutralized surfaces, even in the presence of monovalent counterions.

C. Mixed Systems. In the final part of this work, we study the correlations between two parallel disks of different nature. The first disk is neutral but its surface sites form chemical bond with solvated cations, leading to a net positive electric charge at the disk surface. The cationic affinity of the surface sites is defined by the standard enthalpy of binding: $\Delta_f H° = -80$ kJ/mol.

The second disk bears negatively charged surface sites which also form chemical bond with solvated cations, neutralizing the electric charge of the disk. The affinity of this second set of surface sites is defined by the standard enthalpy of bond formation ($\Delta_f H° = 40$ kJ/mol). Two sets of corresponding indicators are added to monitor the counterions activity. All indicators from the first set are negatively charged and neutralized by forming a chemical bond with solvated monovalent cations ($\Delta_f H° = -45$ kJ/mol). Indicators from the second set are neutral and bind monovalent cations to form electrically charged entities ($\Delta_f H° = -25$ kJ/mol).

The binding process of such mixed systems differs somewhat from our previous results obtained with homogeneous systems (cf. Figures 7 and 8, and 10 and 11). While both ionization (Figure 12a) and neutralization (Figure 12b) processes display

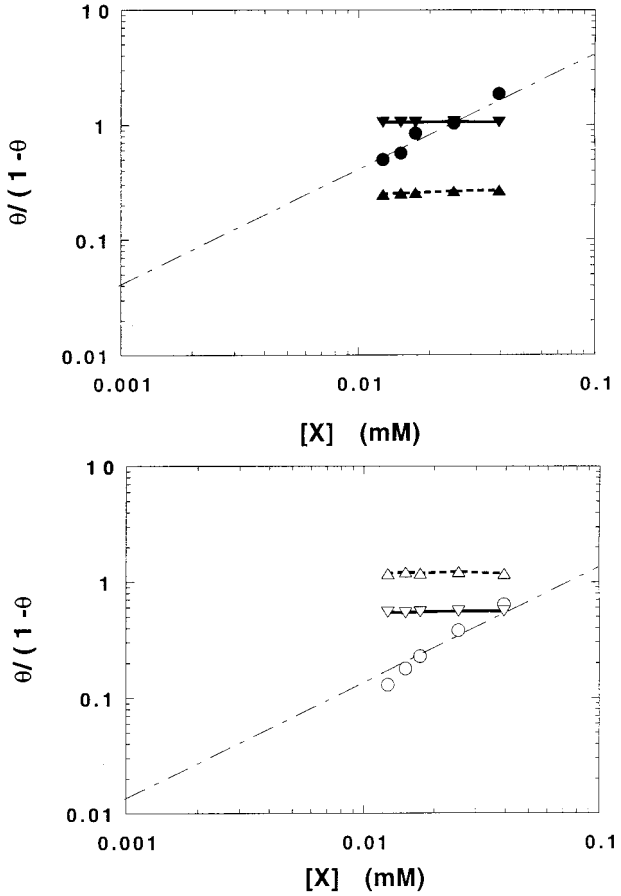

Figure 12. Hill plots describing the degree of binding of a neutral disk and a negatively charged disk facing each other. Both disks bind monovalent cations. The standard enthalpy of binding ($\Delta_i H°$) is −80 kJ/mol for the neutral surface sites (a, top) (▼, inner faces; ▲, outer faces) and −45 kJ/mol for its reference indicators (●). The standard enthalpy of binding is 40 kJ/mol for the negatively charged surface sites (b, bottom) (▽, inner faces; △, outer faces) and −25 kJ/mol for its reference indicators (○) (see text).

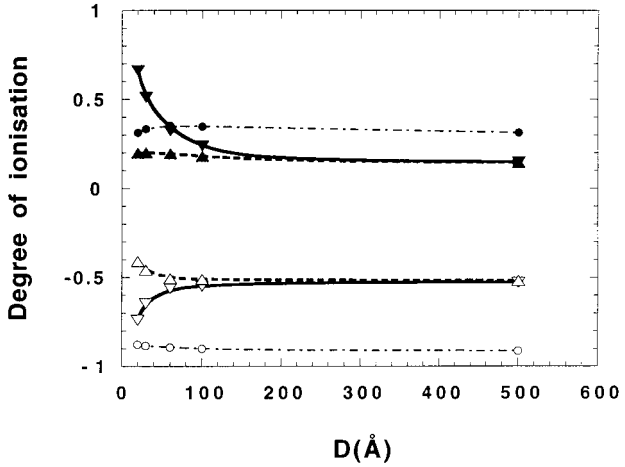

Figure 13. Degree of ionization of one neutral and one negatively charged disk as a function of their separation under the same conditions as for Figure 12.

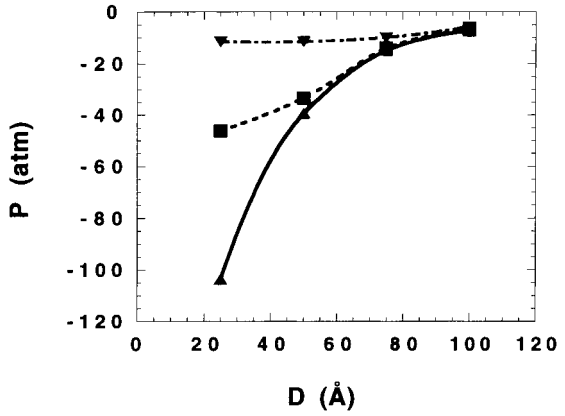

Figure 14. Electrostatic attraction calculated for two asymmetrically charged interfaces, with unifom surface charge density and infinite lateral extent: (▲) $\sigma_1 = 10^{-2}$e/Å^2 and $\sigma_2 = -0.75\sigma_1$; (■) $\sigma_1 = 7.5^{-3}$ e/Å^3 and $\sigma_2 = -0.67\sigma_1$; (▼) $\sigma_1 = 5^{-3}$ e/Å^3 and $\sigma_2 = -0.5\sigma_1$.

strong negative cooperativity, the electrostatic interactions between the disks simultaneously increase the degree of binding of the neutral sites located on the inner surface, as compared to the outer one (Figure 12a), and decrease the degree of binding of the negative sites located on the inner surface, as compared to the outer face (Figure 12b). Note that the opposite behavior was detected for homogeneous systems with either neutral (cf. Figures 7 and 8) or negative (cf. Figures 10 and 11) surfaces sites. In other words, when two cation binding and oppositely charged disks approach each other, the absolute surface charge density of their inner faces increases because of the long-range interionic correlations described by the Monte Carlo formalism. As shown in Figure 13, the amplitude of this phenomenon is 1 order of magnitude larger than in the case of homogeneous systems (cf. Figures 8 and 11).

In order to evaluate the influence of this effect on the colloidal stability, we used Grand Canonical Monte Carlo simulation of the net electrostatic force between two infinite lamellae of opposite and uniform electric charge density,[33,34] in equilibrium with a reservoir of fixed salt concentration ($I = 10^{-4}$ M). As shown in Figure 14, the increase of the absolute value of the surface charge density leads to an enhancement of the long-range electrostatic attraction between the charged colloids.

D. Outlook and Limitations. By performing Monte Carlo simulations of counterion condensation and site binding, we detected asymmetrical degree of binding and ionic condensation of monovalent counterions at inter particle separation lower than 100 Å. This range is expected to increase at lower surface charge density and salt concentration, since both contribute to the local ionic strength which screens the electrostatic interactions between charged colloids. We expect the resulting net attraction to reach the same range (400 Å) and amplitude (∼1 mN/m) as that reported for weakly ionized membranes in salt-free solutions.[70−72]

This conjecture needs, however, to be confirmed by detailed calculations of the electrostatic contribution to the stability of these charged colloids. Indeed, even the sign of the electrostatic force is unknown a priori for these ion binding interfaces, since the modification of the ion distribution in the direct vicinity of the charged colloids (cf. Figure 9, a and b) may deeply alter their electrostatic interaction. We will consider this problem in the near future.

Another question concerns the nature of the electrostatic force between two colloids bearing amphoteric surface sites. Long-range correlation is then expected to occur and organize the surface into patches of sites bearing the same electric charge within a given patch but compensating each other within the same surface. Such patches at the surface of one particle may be located in front of patches of the opposite electric charge on the facing particle. Such inter-site correlations[73−76] should also generate long-range attraction between colloids neutralized by monovalent counterions, even for nearly neutral particles.

IV. Conclusions

We have generalized the Metropolis sampling of the canonical ensemble to describe ion binding in heterogeneous conditions. These Monte Carlo simulations are well suited to describe both ionic condensation on charged surfaces and surface site binding leading to either surface neutralization or ionization. This approach includes all interionic, intersite, and ion−site long-range electrostatic correlations. It predicts the occurrence of different degree of ionization between the inner and outer surfaces of disklike particles at separations lower than 100 Å. We expect this asymmetrical surface ionization to be responsible for attractive electrostatic force between colloids neutralized by monovalent counterions, because of the corresponding asymmetry of counterion condensation.

Acknowledgment. It is a pleasure to cordially thank Dr. E. Perez (ENS, Paris, France) for his interest to the progress of this work and Dr. R. Setton (CRMD, Orleans, France) for interesting discussions. The Monte Carlo simulations were performed on workstations purchased locally thanks to grant from Region Centre (France), on workstations at the Gage Computing Facilities (Ecole Polytechnique, Palaiseau, France), and on Cray supercomputers (IDRIS, Orsay, France).

References and Notes

(1) Attard, Ph. *Adv. Chem. Phys.* **1996**, *92*, 1.
(2) Ninham, B. W. *Adv. Colloid Interface Sci.* **1999**, *83*, 1**.**
(3) Fushiki, M. *J. Chem. Phys.* **1992**, *97*, 6700.
(4) Hug, J. E.; van Swol, F.; Zukoski, C. F. *Langmuir* **1995**, *11*, 111.
(5) Tata, B. V. R.; Ise, N. *Phys. Rev. E* **1998**, *58*, 2237.
(6) Nuesser, W.; Versmold, H. *Mol. Phys.* ***94***, *5*, 759.
(7) Kutter, S.; Hansen, J. P.; Sprik, M.; Boek, E. *J. Chem. Phys.* **2000**, *112*, 311.
(8) Childs, E. C. *Trans. Faraday Soc.* **1954**, *50*, 1356.
(9) Enström, S.; Wennerström, H. *J. Phys. Chem.* **1978**, *82*, 2711.
(10) Delville, A.; Gilboa, H.; Laszlo, P. *J. Chem. Phys.* **1982**, *77*, 2045.
(11) Dubois, M.; Zemb, Th.; Belloni, L.; Delville, A.; Levitz, P.; Setton, R. *J. Chem. Phys.* **1992**, *96*, 2278.
(12) Delville, A. *Langmuir* **1994**, *10*, 395.
(13) Chang, F. R. Ch.; Sposito, G. *J. Colloid Interface Sci.* **1994**, *163*, 19.
(14) McCormack, D.; Carnie, S. L.; Chan, D. Y. C. *J. Colloid Interface Sci.* **1995**, *169*, 177.
(15) Schmitz, K. S. *Langmuir* **1997**, *13*, 5849.
(16) Hsu, J. P.; Tseng, M. T. *Langmuir* **1997**, *13*, 1810.
(17) Mukherjee, A. K.; Bhuiyan, L. B.; Outhwaite, C. W.; Chan, D. Y. C. *Langmuir* **1999**, *15*, 4940.
(18) Neu, J. C. *Phys. Rev. Lett.* **1999**, *82*, 1072.
(19) Outhwaite, C. W.; Bhuiyan, L. B. *J. Chem. Soc., Faraday Trans. 2* **1983**, *79*, 707.
(20) Feller, S. E.; McQuarrie, D. A. *J. Phys. Chem.* **1993**, *97*, 12083.
(21) Elkoubi, D.; Turq, P.; Hansen, J. P. *Chem. Phys. Lett.* **1977**, *52*, 493.
(22) Belloni, L. *J. Chem. Phys.* **1988**, *88*, 5143.
(23) Kjellander, R.; Marcelja, S.; Pashley, R. M.; Quirk, J. P. *J. Phys. Chem.* **1988**, *92*, 6489.
(24) Kjellander, R.; Marcelja, S. *J. Chem. Phys.* **1988**, *88*, 7138.
(25) Meurer, B.; Spegt, P.; Weill, *G. Biophys. Chem.* **1982**, *16*, 89.
(26) Kjellander, R.; Akesson, T.; J6nsson, B.; Maecelja, S. *J. Chem. Phys.* **1992**, *97*, 1424.
(27) Van Megen, W.; Snook, I. *J. Chem. Phys.* **1980**, *7*, 6272.
(28) Guldgrand, L.; J6nsson, B.; Wennerstrom, H.; Linse, P. *J. Chem. Phys.* **1984**, *80*, 2221.
(29) Mills, P.; Anderson, C. F.; Record M. Th., Jr. *J. Phys. Chem.* **1985**, *89*, 3984.
(30) Jayaram, B.; Swaminathan, S.; Beveridge, D. L.; Sharp,K.; Honig, B. *Macromolecules* **1990**, *23*, 3156.
(31) Valleau, J. P.; Ivkov, R.; Torrie, G. M. *J. Chem. Phys.* **1991**, *95*, 520.
(32) Bratko, D.; Henderson, D. *Electrochim. Acta* **1991**, *36*, 1761.
(33) Delville, A.; Pellenq, R. J. M.; Caillol, J. M. *J. Chem. Phys.* **1997**, *106*, 7275.
(34) Pellenq, R. J. M.; Caillol, J. M.; Delville, *A. J. Chem. Phys. B* **1997**, *101*, 8584**.**
(35) Allahyarov, E.; D′Amico, I.; Löwen, H. *Phys. Rev. Lett.* **1998**, *81*, 1334.
(36) Allahyarov, E.; L6wen, H.; Trigger, S. *Phys. Rev. E.* **1998**, *57*, 5818.
(37) Linse, P.; Lobaskin, V. *J. Chem. Phys.* **2000**, *22*, 3917.
(38) Linse, P.; Halle, B. *Mol. Phys.* **1989**, *67*, 537.
(39) Akesson, T.; Jönsson, B. *J. Phys. Chem.* **1985**, *89*, 2401.
(40) Stevens, M. J.; Robbins, M. O. *Europhys. Lett.* **1990**, 81.
(41) Löwen, H.; Madden, P. A.; Hansen, J. P. *Phys. Rev. Lett.* **1992**, *68*, 1081.
(42) Löwen, H.; Hansen, J. P.; Madden, P. A. *J. Chem. Phys.* **1993**, *98*, 3275.
(43) van Roij, R.; Dijkstra, M.; Hansen, J. P. *Phys. Rev. E* **1999**, *59*, 2010.
(44) Patra, Ch. N.; Yethiraj, A. *J. Phys. Chem. B* **1999**, *103*, 6080.
(45) Delville, A. *J. Phys. Chem. B* **1999**, *103*, 8296.
(46) Goodwin, J. W. *Colloidal Dispersions*; The Royal Society of Chemistry: London, 1981; Chapter 3.
(47) Tadros, Th. F. *Solid/Liquid Dispersions*; Academic Press: London, 1987; Chapter 3.
(48) Legrand, P. *The Surfaces Properties of Silica*; John Wiley: New York, 1998.
(49) Delville, A.; Laszlo, P.; Schyns, R. *Biophys. Chem.* **1986**, *24*, 121.
(50) Sposito, G.; Prost, R. *Chem. Rev.* **1982**, *82*, 553.
(51) Low, P. F. *Langmuir* **1987**, *3*, 18.
(52) Cebula, D. J.; Thomas, R. K.; White, J. W. *J. Chem. Soc., Faraday Trans. 1* **1980**, *76*, 314.
(53) Skipper, N. T.; Smalley, M. V.; Williams, G. D.; Soper, A. K.; Thompson, C. H. *J. Phys. Chem.* **1995**, *99*, 14201.
(54) Powell, D. H.; Fischer, H. E.; Skipper, N. T. *J. Phys. Chem. B* **1998**, *102*, 10899.
(55) Poland, D. *Cooperative Equilibria in Physical Biochemistry*; Clarendon Press: Oxford, UK, 1978.
(56) Hayakawa, K.; Kwak, J. C. T. *J. Phys. Chem.* **1982**, *86*, 3866.
(57) Hsu, J. P.; Liu, B. T. *Langmuir* **1999**, *15*, 5219.
(58) Charmas, R. *Langmuir* **1999**, *15*, 5635.
(59) Choi, G. Y.; Kang, J. F.; Ulman, A.; Zurawsky, W. *Langmuir* **1999**, *15*, 8783.
(60) Neto, A. A.; Filho, E. D.; Fossey, M. A.; Neto, J. R. *J. Phys. Chem.* **1999**, *103*, 6809.
(61) Behrens, S. H.; Borkovec, M. *J. Chem. Phys.* **1999**, *111*, 382.
(62) Garces, J. L.; Mas, F.; Puy, J. *J. Chem. Phys.* **1999**, *111*, 2818.
(63) Attard, Ph.; Antelmi, D.; Larson, I. *Langmuir* **2000**, *16*, 1542.
(64) Heyes, D. M. *Phys. Rev. B Condens. Matter* **1994**, *49*, 755.
(65) Hummer, G. *Chem. Phys. Lett.* **1995**, *235*, 297.
(66) Cornish-Bowden, A.; Koshland D. R., Jr. *J. Mol. Biol.* **1975**, *95*, 201.
(67) Israelachvili, J. N. *Intermolecular and Surface Forces*; Academic Press: London, 1985.
(68) Delville, A. *J. Phys. Chem.* **1993**, *97*, 9703.
(69) Delville, A.; Letellier, M. *Langmuir* **1995**, *11*, 1361.
(70) Pincet, F.; Perez, E.; Bryant, G.; Lebeau, L.; Miokowski, Ch. *Phys. Rev. Lett.* **1994**, *73*, 2780.
(71) Pincet, F.; Perez, E.; Bryant, G.; Lebeau, L.; Miokowski, Ch. *Mod. Phys. Lett* **1996**, *10*, 81.
(72) Pincet, F.; Rawicz, W.; Perez, E.; Lebeau, L.; Miokowski, C.; Evans, E. *Phys. Rev. Lett.* **1997**, *79*, 1949.
(73) Rouzina, I.; Bloomfield, V. A. *J. Phys. Chem.* **1996**, *100*, 9977.
(74) Gronbech-Jensen, N.; Mashl, R. J.; Bruinsma, R. F.; Gelbart, W. M. *Phys. Rev. Lett.* **1997**, *78*, 2477.
(75) Ha, B. Y.; Liu, A. J. *Phys. Rev. Lett.* **1997**, *79*, 1289.
(76) Gross, M.; Kiskamp, S. *Phys. Rev. Lett.* **1997**, *79*, 2566.